

---

# EENA: Efficient Evolution of Neural Architecture

---

Hui Zhu<sup>1,2</sup>, Zhulin An<sup>1,\*</sup>, Chuanguang Yang<sup>1</sup>, Kaiqiang Xu<sup>1</sup>, Yongjun Xu<sup>1</sup>

Institute of Computing Technology<sup>1</sup>, University of Chinese Academy of Sciences<sup>2</sup>  
 {zhuhui, Anzhulin, Yangchuanguang, Xukaiqiang, Xuyongjun}@ict.ac.cn

## Abstract

Latest algorithms for automatic neural architecture search perform remarkable but basically directionless in search space and computational expensive in the training of every intermediate architecture. In this paper, we propose a method for efficient architecture search called EENA (Efficient Evolution of Neural Architecture) with mutation and crossover operations guided by the information have already been learned to speed up this process and consume less computational effort by reducing redundant searching and training. On CIFAR-10 classification, EENA using minimal computational resources (0.65 GPU–days) can design highly effective neural architecture which achieves 2.56% test error with 8.47M parameters. Furthermore, The best architecture discovered is also transferable for CIFAR-100.

## 1 Introduction

Convolutional Neural Network has a prominent performance in computer vision, object detection and other fields by extracting features through neural architectures which imitate the mechanism of human brain. Human-designed neural architectures such as ResNet (He et al., 2015), DenseNet (Huang et al., 2016), PyramidNet (Han et al., 2016) and so on which contain several effective blocks are successively proposed to increase the accuracy of image classification. In order to design neural architectures adaptable for various datasets, more researchers have a growing interest in studying the algorithmic solutions based on human experience to achieve automatic neural architecture search (Zoph and Le, 2016; Liu et al., 2017b, 2018; Pham et al., 2018; Cai et al., 2018b, 2019).

Many architecture search algorithms perform remarkable but demand for lots of computational effort. For example, obtaining a state-of-the-art architecture for CIFAR-10 required 7 days with 450 GPUs of evolutionary algorithm (Real et al., 2018) or used 800 GPUs for 28 days of reinforcement learning (Zoph and Le, 2016). The latest algorithms proposed to speed up the process of automatic architecture search, whether based on reinforcement learning (RL) (Pham et al., 2018), sequential model-based optimization (SMBO) (Liu et al., 2017a) and bayesian optimization (Kandasamy et al., 2018) over a discrete search space or based on gradient descent (Liu et al., 2018), neural architecture optimization (NAO) (Luo et al., 2018) over a continuous domain are basically directionless in the search space and computational expensive in the training of every intermediate architecture.

In this work, we propose a method for efficient architecture search called EENA (Efficient Evolution of Neural Architecture) guided by the experience gained in the prior learning to speed up the search process while consume less computational effort. The concept, guidance of experience gained, is inspired by Net2Net (Chen et al., 2015), which generate large networks by transforming small networks via function-preserving. There are several precedents (Cai et al., 2017; Wistuba, 2019) based on this for neural architecture search, but the basic operations are relatively simple and limited to the experience in parameters. We absorb more basic blocks of classical networks, discard several ineffective blocks and even extend the guidance of experience gained to the prior architectures into our method. Due to the loss continue to decrease and the evolution becomes directional, robust and globally optimal models can be discovered rapidly in the search space.

---

\*Corresponding author of this work

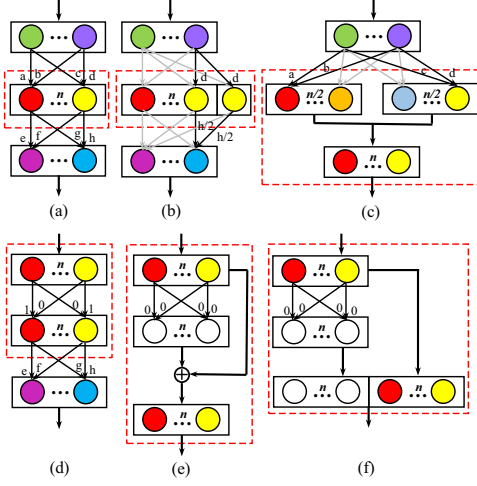


Figure 1: Visualization of the teacher network (a) and several mutation operations (b~f). The rectangles and circles represent the convolution layers and feature maps or filters, respectively. The same color means identical and white means 0 value. The parts in the red dashed box are equivalent.

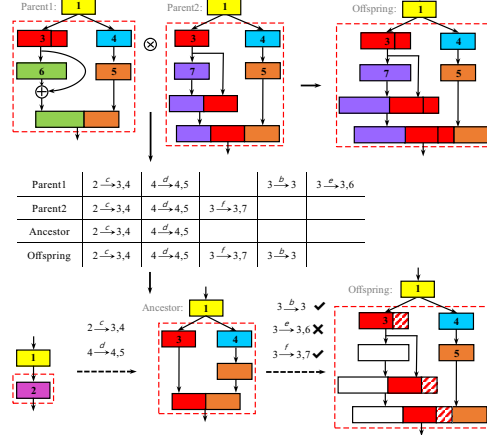


Figure 2: Visualization of the process that the parents produce an offspring by crossover operation. b~f correspond to the mutation operations in Fig. 1 and 1~7 represent the serial number of layers. The same colored rectangles represent the identical layers and white means 0 value. The parts in the red dashed box are equivalent.

Our experiments (Sect. 3) of neural architecture search on CIFAR-10 show that our method using minimal computational resources (0.65 GPU-hours<sup>2</sup>) can design highly effective neural cell that achieves 2.56% test error with 8.47M parameters. We further transfer the best architecture discovered on CIFAR-10 to CIFAR-100 datasets and the results perform remarkable as well.

Our contributions are summarized as follows:

- We are the first to propose crossover operations and improve mutation operations guided by experience gained to effectively reuse the prior learned architectures and parameters.
- We achieve remarkable architecture search efficiency (2.56% error on CIFAR-10 in 0.65 GPU-days) which we attribute to the use of EENA.
- We show that the neural architectures searched by EENA on CIFAR-10 are transferable for CIFAR-100 datasets.

Part of the code implementation and several models we searched on CIFAR-10 of EENA is available at <https://github.com/zhuhui123/EENA>.

## 2 Methods of Efficient Evolution of Neural Architectures

In this section, we illustrate our basic mutation and crossover operations with an example of several connected layers which come from a simple convolutional neural network and describe the method of selection and discard of individuals from the population in the evolution process.

### 2.1 Search space and mutation operations.

The birth of a better network architecture is usually achieved based on local improvements. Chollet (2016) proposes to replace Inception with depthwise separable convolutions to reduce the number of parameters. Grouped convolutions given by Krizhevsky et al. (2012) is used to distributing the model over two GPUs and Xie et al. (2016) further proposes that increasing cardinality is more effective than going deeper or wider based on this. He et al. (2015) solves the degradation problem

<sup>2</sup>All of our experiments were performed using a NVIDIA Titan Xp GPU.

of deep neural networks by residual blocks. Huang et al. (2016) proposes dense blocks to solve the vanishing-gradient problem, strengthen feature propagation and substantially reduce the number of parameters. Some of the existing methods (Chen et al., 2015; Wistuba, 2019) based on function-preserving are briefly reviewed in this section and the guidance of experience gained in parameters is built on them. Specifically, we absorb more blocks of classical networks such as dense block, add some effective changes such as noises for new parameters and discard several ineffective operations such as kernel widening in our method.

The search space of our method consists of all the basic mutation operations and every mutation refers to a random change for an individual.  $x$  is the input to the network, the guidance of experience gained in parameters is to choose a new set of parameters  $\theta'$  for a student network  $g(x; \theta')$  which transform from the teacher network  $h(x; \theta)$  such that  $\forall x : h(x; \theta) = g(x; \theta')$ <sup>3</sup>. Assume that the  $i$ -th convolutional layer to be changed is represented by a  $(k_1, k_2, c, f)$  shaped matrix  $W^{(i)}$ . The input for the convolution operation in layer  $i$  is represented as  $X^{(i)}$  and the processing of BatchNorm and other layers is expressed as  $\varphi$ . In this work, we consider the following mutation operations.

**Widen a layer.** Fig. 1(b) is an example of this operation.  $W^{(i)}$  is extend by replicating the parameters along the last axis at random and the parameters in  $W^{(i+1)}$  need to be divided along the third axis corresponding to the counts of the same filters in the  $i$ -th layer. Specifically, A 0 to 5e-2 times noise  $\delta$  is randomly added to every new parameter in  $W^{(i+1)}$  to break symmetry.

$$g(j) = \begin{cases} j & j \leq f \\ \text{random sample from } \{1, 2, \dots, f\} & j > f \end{cases}.$$

$$U_{k_1, k_2, c, j}^{(i)} = W_{k_1, k_2, c, g(j)}^{(i)}, \quad U_{k_1, k_2, j, f}^{(i+1)} = \frac{1}{\text{card}(x|g(x)=g(j))} W_{k_1, k_2, g(j), f}^{(i+1)} + \delta.$$

**Branch a layer.** Fig. 1(c) is an example of this operation.  $U$  and  $V$  are the new parameter matrices. This operation adds no further parameters and will always be combined with other operations.

$$U_{k_1, k_2, c, j}^{(i)} = W_{k_1, k_2, c, m}^{(i)} \quad m \in \left[0, \lfloor \frac{f}{2} \rfloor\right], \quad V_{k_1, k_2, c, l}^{(i)} = W_{k_1, k_2, c, m}^{(i)} \quad m \in \left(\lfloor \frac{f}{2} \rfloor, f\right].$$

$$\text{Operation\_output} = \text{Concatenate} \left( \varphi \left( X^{(i)} \cdot U_{k_1, k_2, c, j}^{(i)} \right), \varphi \left( X^{(i)} \cdot V_{k_1, k_2, c, l}^{(i)} \right) \right).$$

**Insert a single layer.** Fig. 1(d) is an example of this operation. The new layer weight matrix  $U^{(i+1)}$  with a  $k_1 \times k_2$  kernel is initialized to an identity matrix and  $\text{ReLU}(x) = \max\{x, 0\}$  satisfies the restriction for the activation function  $\sigma$ :  $\forall x : \sigma(x) = \sigma(I\sigma(x))$ .

$$U_{j, l, a, b}^{(i+1)} = \begin{cases} 1 & j = \frac{k_1+1}{2} \wedge l = \frac{k_2+1}{2} \wedge a = b \\ 0 & \text{otherwise} \end{cases}.$$

**Insert a layer with shortcut connection.** Fig. 1(e) is an example of this operation. All the parameters of the new layer weight matrix  $U^{(i+1)}$  are initialized to 0.

$$\text{Operation\_output} = \text{ReLU} \left( \text{Add} \left( X^{(i+1)}, X^{(i+1)} \cdot U^{(i+1)} \right) \right).$$

**Insert a layer with dense connection** Fig. 1(f) is an example of this operation. All the parameters of the new layer weight matrix  $U^{(i+1)}$  are initialized to 0.

$$\text{Operation\_output} = \text{Concatenate} \left( \varphi \left( X^{(i+1)} \cdot U^{(i+1)} \right), \varphi \left( X^{(i+1)} \right) \right).$$

**Other mutations.** In addition, many other important methods, such as separable convolution, grouped convolution, bottleneck, widening the kernel etc., all can be absorbed into the mutation operations. In order to making a balance between the number of parameters and the accuracy of classification, we eventually abandon these operations in our experiment.

<sup>3</sup>The '=' here doesn't mean completely equivalent, noise may be added to make the student more robust.

## 2.2 Crossover operations.

As the focus of our method, crossover refers to the combination of the prominent parents to produce offsprings which may perform even more excellent. The parents refer to the architectures with high fitness that have been already discovered and every offspring is the new exploration of the search space. Obviously, although our mutation operations reduce the computational effort of the repeated retraining, the exploration of the search space is still random without taking advantage of the experience already gained in prior architectures. The crossover operations can effectively reuse the parameters already trained and even produce the next generation guided by experience of the prior excellent architectures. The crossover operations in this work mainly includes:

- Inheriting the whole architecture of individual A with the highest fitness and randomly adding the different parts of the architecture of individual B to A.
- Inheriting the same architecture of the two individuals with high fitness and the offsprings randomly inherit the different parts of architectures of the parents.
- Scanning the architectures of several individuals with high fitness and the inherited probability of architectures with high proportion of all is correspondingly large.
- Combine the architecture with each other in the same location of several networks by Add or Concatenate operations.

Although all the methods are effective, we adopt the second method mentioned above in our final reported experiments considering of the limits on the number of parameters. Fig. 2 is a visual example of the second crossover operation. Based on the records about the previous mutation operations for each individual (for Parent1, mutation c, d, b, e occurred at layer 2, 4, 3, 3, respectively and for Parent2, mutation c, d, f occurred at layer 2, 4, 3, respectively), the common ancestor of the parents (Ancestor with mutation c, d occurred at layer 2, 4) can be easily found. The mutation operations of the two parents different from each other are selected and added to the ancestor architecture according to a certain probability by the mutation operations (mutation b, f occurred at layer 3, 3 are inherited by Offspring and mutation e is randomly discarded).

## 2.3 The selection and discard of individuals in evolutionary algorithm

**The selection of Individuals.** Our evolutionary algorithm uses tournament selection (Goldberg and Deb, 1991) to select an individual for mutation: a fraction  $k$  of individuals is selected from the population randomly and the individual with highest fitness is final selected from this set. For crossover, the two individuals with the highest fitness but different architectures will be selected.

**The discard of Individuals.** In order to constrain the size of the population, the discard of individuals will be accompanied by the generation of each new individual when the population size reaches  $N$ . We regulate aging and non-aging evolutions (Real et al., 2018) via the variable  $\lambda$  to affect the convergence rate and overfit: Discarding the worst model with  $\lambda$  probability and the oldest model with  $1 - \lambda$  within each round.

## 3 Experiments

In this section, we report the performances of EENA in neural architecture search on CIFAR-10 and the feasibility of transferring the best architecture discovered on CIFAR-10 to CIFAR-100. In our experiments, we start the evolution from initializing a simple convolutional neural network to show the efficiency of EENA and we use the methods of selection and discard mentioned in (Sect. 2.3) to select individuals from the population and the mutation (Sect. 2.1) and crossover (Sect. 2.2) operations to improve the neural architectures.

**Initial model.** The initial model (the number of parameters is 0.67M) is sketched in Figure 3. It starts with one convolution and then three evolutionary blocks and two MaxPooling layers for down-sampling are connected alternately. Then another convolution is added, followed by a GlobalAveragePooling layer and a Softmax layer for transformation from feature map to classification. Each MaxPooling layer has a stride of two and is followed by a DropBlock (Ghiasi et al., 2018) layer

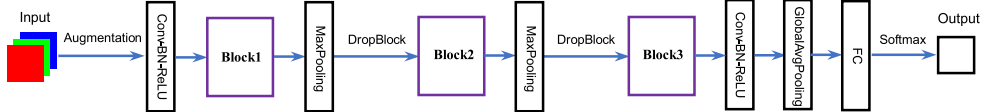


Figure 3: The initial model designed in our experiments.

with  $keep\_prob = 0.8$  ( $block\_size = 7$  for the first one and  $block\_size = 5$  for the second one). Specifically, the first convolution contains 64 filters and the last convolution contains 256 filters. An evolutionary block is initialized with a convolution with 128 filters. Every convolutional layer mentioned actually means a Conv-BatchNorm-ReLU block with a kernel size of  $3 \times 3$ . The weights are initialized as He normal distribution (He et al., 2015) and the L2 regularization of 0.0001 is applied to the weights.

**Dataset.** We randomly sample 10,000 images by stratified sampling from the original training set to form a validation set for evaluate the fitness of the individuals while using the remaining 40,000 images for training the individuals during the evolution. We normalize the images using channel means and standard deviations for preprocessing and apply a standard data augmentation scheme (zero-padding with 4 pixels on each side to obtain a  $40 \times 40$  pixels image, then randomly cropping it to size  $32 \times 32$  and randomly flipping the image horizontally).

**Search on CIFAR-10.** The initial population consists of 12 individuals, each formed by a single mutation operation from the common initial model. During the process of evolution, Individual selection is determined by the fitness (accuracy) of the neural architecture evaluated on the validation set. In our experiments, the size of  $k$  in selection of individuals is fixed to 3 and the variable  $\lambda$  in discard of individuals is fixed to 0.5. We don't discard any individual at the beginning to make the population grow to the size of 20. Then we use selection and discard together, that is to say, the individual after mutation or crossover operations will be put back into the population after training and at the same time the discard of individuals will be executed. The mutation and crossover operations to improve the neural architectures can be applied anywhere in the evolutionary block and any mutation operation is selected by the same probability. The crossover operation is executed every 5 rounds, for which we select the two individuals as parents with the highest fitness but different architectures among the population. All the neural architectures are trained with a batch size of 128 using SGDR (Loshchilov and Hutter, 2016) with initial learning rate  $l_{max} = 0.05$ ,  $T_0 = 1$  and  $T_{mult} = 2$ . The initial model is trained for 63 epochs. Then, 15 epochs are trained after each mutation operation, one round of 7 epochs and another round of 15 epochs are trained after each crossover operation. We keep recording the best fitness of the population and other important information. One search process on CIFAR-10 is visualized in figure 4. In the circle phylogenetic tree of EENA, the color of the outermost circle represents fitness, and the same color of the penultimate circle represents the same ancestor. In the rectangular phylogenetic tree, the color on the right side represents fitness. From the inside to the outside in the left figure and from left to right in the right figure, along the direction of time axis, the connections represent the relationship from ancestors to offsprings. We can notice that the fitness of the population increases steadily and rapidly via mutation and crossover operations guided by experience gained. In addition, the population is quickly taken over by a highly performing homologous group. After the search budget is exhausted or the highest fitness of the population doesn't increase over 25 rounds, the individual with highest fitness will be extracted as the best neural architecture for post-training.

**Post-training of the best neural architecture obtained.** We conduct post-processing and post-training towards the best neural architecture designed by the EENA. The model is trained on the full training dataset until convergence using Cutout (Devries and Taylor, 2017) and Mixup (Zhang et al., 2017) whose configurations are the same as the original paper (a cutout size of  $16 \times 16$  and  $\alpha = 1$  for mixup). Specifically, in order to reflect the fairness of the result for comparison, we don't use the latest method proposed by Cubuk et al. (2018) which has significant effects but hasn't been widely used yet. The neural architectures are trained with a batch size of 128 using SGDR (Loshchilov and Hutter, 2016) with initial learning rate  $l_{max} = 0.1$ ,  $T_0 = 1$  and  $T_{mult} = 2$  for

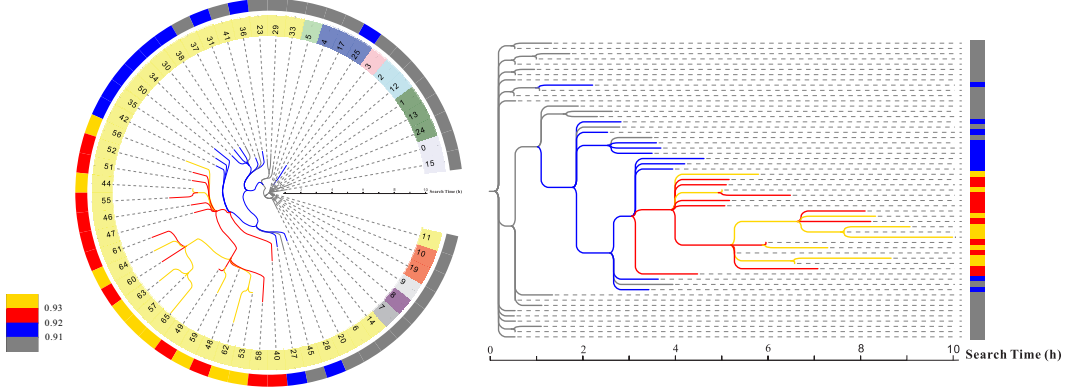


Figure 4: The phylogenetic tree visualized one search process on CIFAR-10. In the circle phylogenetic tree, the color of the outermost circle represents fitness, and the color of the penultimate circle represents ancestor. In the rectangular phylogenetic tree, the color on the right side represents fitness. From the inside to the outside in the left figure and from left to right in the right figure, along the direction of time axis, the relationship represents from ancestors to offsprings.

Table 1: Comparison against state-of-the-art recognition results on CIFAR-10. Results marked with  $\dagger$  are NOT trained with Cutout (Devries and Taylor, 2017). The first block represents the performance of human-designed architectures. The second block represents results of various automatically designed architectures. Our method use minimal computational resources to achieve a low test error.

Method	Params (Mil.)	Search Time (GPU-days)	Test Error (%)
DenseNet-BC (Huang et al., 2016) $\dagger$	25.6	—	3.46
PyramidNet-Bottleneck (Han et al., 2016) $\dagger$	26.0	—	3.31
ResNeXt + Shake-Shake (Gastaldi, 2017) $\dagger$	26.2	—	2.86
AmoebaNet-A (Real et al., 2018)	3.2	3150	3.34
Large-scale Evolution (Real et al., 2017) $\dagger$	5.4	2600	5.4
NAS-v3 (Zoph and Le, 2016)	37.4	1800	3.65
NASNet-A (Zoph et al., 2017)	3.3	1800	2.65
Hierarchical Evolution (Liu et al., 2017b) $\dagger$	15.7	300	3.75
PNAS (Liu et al., 2017a) $\dagger$	3.2	225	3.41
Path-Level-EAS (Cai et al., 2018b)	14.3	200	2.30
NAONet (Luo et al., 2018)	128	200	2.11
EAS (Cai et al., 2018a) $\dagger$	23.4	10	4.23
DARTS (Liu et al., 2018)	3.4	4	2.83
Neuro-Cell-based Evolution (Wistuba, 2019)	7.2	1	3.58
ENAS (Pham et al., 2018)	4.6	0.45	2.89
NAC (Kamath et al., 2018)	10	0.25	3.33
Ours	7.18	0.56	2.76
Ours	8.47	0.65	2.56

511 or 1023 epochs<sup>4</sup>. Finally, the error on the test dataset is reported. The comparison against state-of-the-art recognition results on CIFAR-10 is presented in Table 1. On CIFAR-10, Our method using minimal computational resources (0.65 GPU-days) can design highly effective neural cell that achieves 2.56% test error with small number of parameters (8.47M).

**Transfer the best cell searched on CIFAR-10 to CIFAR-100.** We further try to transfer the best cell of highest fitness searched on CIFAR-10 to CIFAR-100 and the results perform remarkable

<sup>4</sup>We did not conduct extensive hyperparameter tuning due to limited computation resources.

Table 2: Comparison against state-of-the-art recognition results on CIFAR-100. The first block represents the performance of human-designed architectures. The second block represents the results of several automatically designed architectures. The last block represents the performance of transferring the best architecture discovered on CIFAR-10 to CIFAR-100.

Method	Params (Mil.)	Search Time (GPU-days)	Test Error (%)
DenseNet-BC (Huang et al., 2016)	25.6	—	17.18
ResNeXt + Shake-Shake (Gastaldi, 2017)	26.2	—	15.20
AmoebaNet-B (Real et al., 2018)	34.9	3150	15.80
Large-scale Evolution (Real et al., 2017)	40.4	2600	23.70
NASNet-A (Zoph et al., 2017)	50.9	1800	16.03
PNAS (Liu et al., 2017a)	3.2	225	17.63
NAONet (Luo et al., 2018)	128	200	14.75
Neuro-Cell-based Evolution (Wistuba, 2019)	5.3	1	21.74
ENAS (Pham et al., 2018)	4.6	0.45	17.27
Ours (transferred from CIFAR-10)	8.49	—	17.78

as well. For CIFAR-100, several hyper-parameters are modified:  $block\_size = 4$  for the first DropBlock layer,  $block\_size = 3$  for the second and the cutout size is  $8 \times 8$ . The comparison against state-of-the-art recognition results on CIFAR-100 is presented in Table 2.

## 4 Conclusions and Ongoing Work

We design an efficient method of neural architecture search based on evolution with the guidance of experience gained in the prior learning. This method takes repeatable network blocks (cells) as the basic units for evolution, and achieves a state-of-the-art accuracy on CIFAR-10 and others with few parameters and little search time. We notice that the initial model and the basic operations are extremely impactful to search speed and final accuracy. Therefore, we are trying to add several effective blocks such as grouped convolution as mutation operations combined with other methods that might perform effective such as macro-search (Hu et al., 2018) into our experiments.

## References

Han Cai, Tianyao Chen, Weinan Zhang, Yong Yu, and Jun Wang. Reinforcement learning for architecture search by network transformation. *CoRR*, abs/1707.04873, 2017. URL <http://arxiv.org/abs/1707.04873>.

Han Cai, Tianyao Chen, Weinan Zhang, Yong Yu, and Jun Wang. Efficient architecture search by network transformation. 04 2018a.

Han Cai, Jiacheng Yang, Weinan Zhang, Song Han, and Yong Yu. Path-level network transformation for efficient architecture search. *CoRR*, abs/1806.02639, 2018b. URL <http://arxiv.org/abs/1806.02639>.

Han Cai, Ligeng Zhu, and Song Han. ProxylessNAS: Direct neural architecture search on target task and hardware. In *International Conference on Learning Representations*, 2019. URL <https://openreview.net/forum?id=HylVB3AqYm>.

Tianqi Chen, Ian Goodfellow, and Jonathon Shlens. Net2net: Accelerating learning via knowledge transfer. 11 2015.

François Chollet. Xception: Deep learning with depthwise separable convolutions. *CoRR*, abs/1610.02357, 2016. URL <http://arxiv.org/abs/1610.02357>.

Ekin Dogus Cubuk, Barret Zoph, Dandelion Mané, Vijay Vasudevan, and Quoc V. Le. Autoaugment: Learning augmentation policies from data. *CoRR*, abs/1805.09501, 2018. URL <http://arxiv.org/abs/1805.09501>.

Terrance Devries and Graham W. Taylor. Improved regularization of convolutional neural networks with cutout. *CoRR*, abs/1708.04552, 2017. URL <http://arxiv.org/abs/1708.04552>.

Xavier Gastaldi. Shake-shake regularization. *CoRR*, abs/1705.07485, 2017. URL <http://arxiv.org/abs/1705.07485>.

Golnaz Ghiasi, Tsung-Yi Lin, and Quoc V. Le. Dropblock: A regularization method for convolutional networks. *CoRR*, abs/1810.12890, 2018. URL <http://arxiv.org/abs/1810.12890>.

David E. Goldberg and Kalyanmoy Deb. A comparative analysis of selection schemes used in genetic algorithms. volume 1 of *Foundations of Genetic Algorithms*, pages 69 – 93. Elsevier, 1991. doi: <https://doi.org/10.1016/B978-0-08-050684-5.50008-2>. URL <http://www.sciencedirect.com/science/article/pii/B9780080506845500082>.

Dongyoon Han, Jiwhan Kim, and Junmo Kim. Deep pyramidal residual networks. *CoRR*, abs/1610.02915, 2016. URL <http://arxiv.org/abs/1610.02915>.

Kaiming He, Xiangyu Zhang, Shaoqing Ren, and Jian Sun. Deep residual learning for image recognition. *CoRR*, abs/1512.03385, 2015. URL <http://arxiv.org/abs/1512.03385>.

Hanzhang Hu, John Langford, Rich Caruana, Eric Horvitz, and Debadatta Dey and. Macro neural architecture search revisited. 2018.

Gao Huang, Zhuang Liu, and Kilian Q. Weinberger. Densely connected convolutional networks. *CoRR*, abs/1608.06993, 2016. URL <http://arxiv.org/abs/1608.06993>.

Purushotham Kamath, Abhishek Singh, and Debo Dutta. Neural architecture construction using envelopenets. *CoRR*, abs/1803.06744, 2018. URL <http://arxiv.org/abs/1803.06744>.

Kirthevasan Kandasamy, Willie Neiswanger, Jeff Schneider, Barnabás Póczos, and Eric Xing. Neural architecture search with bayesian optimisation and optimal transport. *CoRR*, abs/1802.07191, 2018. URL <http://arxiv.org/abs/1802.07191>.

Alex Krizhevsky, Ilya Sutskever, and Geoffrey E Hinton. Imagenet classification with deep convolutional neural networks. In F. Pereira, C. J. C. Burges, L. Bottou, and K. Q. Weinberger, editors, *Advances in Neural Information Processing Systems 25*, pages 1097–1105. Curran Associates, Inc., 2012. URL <http://papers.nips.cc/paper/4824-imagenet-classification-with-deep-convolutional-neural-networks.pdf>.

Chenxi Liu, Barret Zoph, Jonathon Shlens, Wei Hua, Li-Jia Li, Li Fei-Fei, Alan L. Yuille, Jonathan Huang, and Kevin Murphy. Progressive neural architecture search. *CoRR*, abs/1712.00559, 2017a. URL <http://arxiv.org/abs/1712.00559>.

Hanxiao Liu, Karen Simonyan, Oriol Vinyals, Chrisantha Fernando, and Koray Kavukcuoglu. Hierarchical representations for efficient architecture search. *CoRR*, abs/1711.00436, 2017b. URL <http://arxiv.org/abs/1711.00436>.

Hanxiao Liu, Karen Simonyan, and Yiming Yang. DARTS: differentiable architecture search. *CoRR*, abs/1806.09055, 2018. URL <http://arxiv.org/abs/1806.09055>.

Ilya Loshchilov and Frank Hutter. SGDR: stochastic gradient descent with restarts. *CoRR*, abs/1608.03983, 2016. URL <http://arxiv.org/abs/1608.03983>.

Renqian Luo, Fei Tian, Tao Qin, and Tie-Yan Liu. Neural architecture optimization. *CoRR*, abs/1808.07233, 2018. URL <http://arxiv.org/abs/1808.07233>.

Hieu Pham, Melody Y. Guan, Barret Zoph, Quoc V. Le, and Jeff Dean. Efficient neural architecture search via parameter sharing. *CoRR*, abs/1802.03268, 2018. URL <http://arxiv.org/abs/1802.03268>.

Esteban Real, Sherry Moore, Andrew Selle, Saurabh Saxena, Yutaka Leon Suematsu, Quoc V. Le, and Alex Kurakin. Large-scale evolution of image classifiers. *CoRR*, abs/1703.01041, 2017. URL <http://arxiv.org/abs/1703.01041>.

Esteban Real, Alok Aggarwal, Yanping Huang, and Quoc V. Le. Regularized evolution for image classifier architecture search. *CoRR*, abs/1802.01548, 2018. URL <http://arxiv.org/abs/1802.01548>.

Martin Wistuba. Deep learning architecture search by neuro-cell-based evolution with function-preserving mutations. In Michele Berlingerio, Francesco Bonchi, Thomas Gärtner, Neil Hurley, and Georgiana Ifrim, editors, *Machine Learning and Knowledge Discovery in Databases*, pages 243–258, Cham, 2019. Springer International Publishing. ISBN 978-3-030-10928-8.

Saining Xie, Ross B. Girshick, Piotr Dollár, Zhuowen Tu, and Kaiming He. Aggregated residual transformations for deep neural networks. *CoRR*, abs/1611.05431, 2016. URL <http://arxiv.org/abs/1611.05431>.

Hongyi Zhang, Moustapha Cissé, Yann N. Dauphin, and David Lopez-Paz. mixup: Beyond empirical risk minimization. *CoRR*, abs/1710.09412, 2017. URL <http://arxiv.org/abs/1710.09412>.

Barret Zoph and Quoc V. Le. Neural architecture search with reinforcement learning. *CoRR*, abs/1611.01578, 2016. URL <http://arxiv.org/abs/1611.01578>.

Barret Zoph, Vijay Vasudevan, Jonathon Shlens, and Quoc V. Le. Learning transferable architectures for scalable image recognition. *CoRR*, abs/1707.07012, 2017. URL <http://arxiv.org/abs/1707.07012>.